



4-1981

The Effect of High Frequency Sinusoidal Strains on the Strength Properties of Paper

Robert McQueary
Western Michigan University

Follow this and additional works at: <https://scholarworks.wmich.edu/engineer-senior-theses>



Part of the Wood Science and Pulp, Paper Technology Commons

Recommended Citation

McQueary, Robert, "The Effect of High Frequency Sinusoidal Strains on the Strength Properties of Paper" (1981). *Paper Engineering Senior Theses*. 328.
<https://scholarworks.wmich.edu/engineer-senior-theses/328>

This Dissertation/Thesis is brought to you for free and open access by the Chemical and Paper Engineering at ScholarWorks at WMU. It has been accepted for inclusion in Paper Engineering Senior Theses by an authorized administrator of ScholarWorks at WMU. For more information, please contact wmu-scholarworks@wmich.edu.



THE EFFECT OF HIGH FREQUENCY SINUSOIDAL
STRAINS ON THE STRENGTH PROPERTIES OF PAPER

By

Robert McQueary

A Thesis submitted in partial fulfillment of
the course requirement for The Bachelor of Science Degree

Western Michigan University

Kalamazoo, Michigan

April, 1981

ABSTRACT

The objective of this study was to determine the effect of various high frequency sinusoidal strains on the strength properties of a paper cone in a loud speaker. The stresses developed during sound propagation were approximated by applying viscoelastic theories to the paper cone's mode of response. This analysis indicated the stresses developed would be indirectly proportional to the square of the frequency in Hertz. Also relevant is the Boltzmann superposition principle which states that if a second strain is applied before the first strain is dissipated, the resultant strains are additive.

Sets of speakers were operated continuously for 120 hours at three different frequencies: 100, 1K and 10K Hertz. The power supplied remained constant. An increase in the results of the elongation, folding endurance, TEA and tensile tests and a decrease in the stiffness tests were observed at each frequency. The results indicate that the larger applied shear strain causes a larger variance in the test results. The 10K Hz set yielded a larger variance than the 1K Hz set, implying that the Boltzmann superposition principle is applicable at the higher frequency.

Future work should consider operating speakers for longer time periods and include higher frequencies. These studies could generate more knowledge on the mode of failure and possibly when the added strains would cause a decrease in strength properties that could effect the cone's ability to produce undistorted sound. The extended operation of the speakers could also be compared with the operation of speakers that have been artificially aged to give more insight to the mechanisms of aging.

TABLE OF CONTENTS

	Page
INTRODUCTION	1
HISTORICAL BACKGROUND	2
EXPERIMENTAL PROCEDURE	5
RESULTS PRESENTATION	7
DISCUSSION OF RESULTS	10
CONCLUSIONS	13
RECOMMENDATIONS	14
LITERATURE CITED	15
APPENDIX I Speaker Components	16
APPENDIX II Derivation of Shear Stress	17
APPENDIX III Derivation of Sinusoidally Applied Shear Stress	20
APPENDIX IV The Relationship of Shear Strain to Tensile Strain	24
APPENDIX V Experimental Procedure	25
APPENDIX VI Exploratory Experimentation Test Results	30
APPENDIX VII Primary Experimentation Test Results	32

INTRODUCTION

The ability to evaluate paper with relevant test procedures to predict its ultimate capabilities in its end use application is required to establish quality standards. Whenever tests can not accurately simulate the mode of failure, approximations are made. Presently, paper loud speaker cone manufacturers must assemble the speaker before any quality tests can be run. One manufacturer tests assembled drivers at one middle frequency with increasing power until the cone is "blown". Failure occurs when the cone no longer maintains its structural integrity or the voice coil is incapable of properly moving the cone. For a description of a driver and its components see Appendix I.

If the mode of failure or the detrimental effects from operation could be determined, the fibers could be prepared differently to alter the structure of the cone to reduce the effects of operation. The difference in preparation could vary from the type of refining to the use of chemical additives before or after formation of the cone. The preparation could change the flexibility of the fibers or the bonds, depending on the structural needs of the cone. The analysis of the stresses produced during operation and the determination of the structural changes caused by operation would increase the knowledge of the mechanisms of the cone's failure.

This thesis will investigate the effects of operating with various sinusoidal frequencies on the strength properties of tensile, TEA, elongation, folding endurance and stiffness of a cone. The tensile and shear forces developed in a paper cone during sound propagation will be approximated by applying visco-elastic theories to the response of a cone to the applied strains. The frequency inducing the largest forces should cause the highest loss of strength properties.

HISTORICAL BACKGROUND

Before the theories of viscoelastic behavior of materials can be applied to an operating cone, it should be shown to be capable of responding as a viscoelastic substance. A definition of viscoelastic substance would first be appropriate. A viscoelastic substance exhibits a mode of response similar to a viscous liquid and an elastic solid. The method of analysis used here is based on the energy dissipation of an operating driver.

The energy used by a driver is dissipated by several methods. The most obvious mode is the sound produced. The changes in the magnetic flux in and the movement of the voice coil causes the magnet to increase in temperature and is another use of energy. Energy is used to reverse the momentum of the cone, voice coil and voice coil form. The temperature of the fibers in the cone could increase and dissipate energy to its surroundings. Also, the cone can bend and absorb energy. The distortion of a cone can readily be observed with a strobe light on an operating cone. It is this apparent mode of energy dissipation that will be investigated further.

The ability of the cone to deform and thereby absorb energy, indicates that it is capable of straining and distributing stresses at a sonic rate. The stresses developed at the apex are greater because there is less area to distribute the stresses per given distance of the radius and less energy has been dissipated. This indicates that the paper cone in operation exhibits the behavior of a viscoelastic material. Previously, the understanding of the rheology of paper has been improved by the application of viscoelastic principles. Horio and Onogi et al. (1,2,3) have used these principles to approximate the complex Young's Modulus.

To facilitate the explanation of forces developed in viscoelastic materials, stress, strain and modulus should be explained. An external force applied to

a body is a stress. The deformation caused by the applied stress is called strain. The relationship between stress and strain is the modulus. It is now possible to develop the modulus in a cone.

Assuming paper in the cone exhibits a mode of response of a viscoelastic material, the strain developed while producing a single frequency should be approximated by using an equation for sinusoidally applied shear stress. Appendix II provides a development of shear stress in a viscoelastic body. Ferry(4) has shown that the sinusoidally applied shear stress (σ_{21}) can be calculated by the following equation:

$$\sigma_{21} = \gamma (G' \sin \omega t + G'' \cos \omega t) \quad (1)$$

Where: γ = maximum amplitude of strain

σ_{21} = shear stress

ω = frequency (radians 1 second)

G' = shear storage modulus

G'' = shear loss modulus

To evaluate the stress equally for all frequencies, the integral will be solved for one-half a period and multiplied by twice the frequency in hertz. This will give the absolute value of compressional and tensional stresses during a one second time period. Since the power input will be equivalent, the amplitude is proportional to the inverse of the frequency squared. The shear and tensile stresses are proportional to the amplitude and therefore the stress equations indicate that the lowest frequency causes the highest shear stress. For a complete derivation of the sinusoidally applied shear stress see Appendix III.

Ferry's equation implies that shear rate is the controlling factor of strength variance. Barkas(5) tested paper under different pre-straining loading cycles and concluded the largest loss of tensile was experienced with the highest loading rate. This agrees with the Boltzmann super position principle which

states that a second stress (also any other discrete stresses) produces a strain that is additive to the first. Assuming that the second strain is applied before the first strain can be dissipated, the highest frequencies would compound strains at a rate proportional to the cycles per second. Using the previous assumption, a 5K Hz note from the cone would cause a force 50 times that of a 100 Hz note. Since most speaker cones rupture playing low frequencies, (6) it is improbable that the high frequency strains accumulate to produce a larger stress than the lower frequencies.

Therefore, the assumption that the paper cone is capable of dissipating the strains applied, even at the higher frequencies is acceptable. Then, the rate of shear is of lesser importance to the strength loss in the cones.

However, it is possible that both could be occurring at the same time and yield a result in between the two previous hypotheses. This would mean that somewhere in the sonic frequencies the paper would be incapable of distributing the first stress before a second was applied. Moreover, this could happen several times before the shear stress from the higher frequency exceeded that from the lower frequency. If the shear stress analysis is true, the frequency at which the strains are not dissipated would be where the strength loss increases with higher frequencies.

EXPERIMENTAL PROCEDURE

The five inch diameter drivers used were donated by Carbonneau Industries of Grand Rapids. They were manufactured for use in 3M tape recorders. The recorders were used for primary and secondary education in classrooms. The maximum recommended power input is 10 Watts (W)_{rms}.

EXPLORATORY EXPERIMENT

Three drivers were aged in an oven at 105°C to simulate 25 years of natural aging. A fourth driver was placed with the aged drivers in the test chamber. They were allowed to equilibrate to the 40% RH air before operation. The originally planned frequencies of operation were picked at 100, 1000 and 10K hertz (Hz) because they were within the expected operational range of these drivers and represent a low, middle and high frequency note. Because of the limited number of drivers, the exploratory experimentation used 100 and 10K Hz only.

A signal generator connected to an amplifier provided the power to the driver being operated. The power was calculated daily by dividing the square of the voltage drop across the driver by the dynamic resistance of the driver measured at 1K Hz. The drivers were operated at 9 W_{rms} continuously for 120 hours mounted on a near vertical board.

After the operation was completed, the four drivers were placed in a humidity controlled paper testing room which was kept at 60% RH. Four tensile and fold specimens were cut from each driver and tested. Since fold specimens were under one inch long, scotch tape was used to extend the specimen from the jaw to the clamp.

PRIMARY EXPERIMENTATION

All drivers were placed in the testing chamber and allowed to equilibrate

to the 40% RH air. During the operation of the drivers, three parallel branches were made using two drivers in series. Since only enough drivers were obtained to allow five drivers per frequency, a previously used driver was taped (to replace the removed paper) and used to complete the electronic circuit. The drivers were mounted on a plywood board which tilted slightly backwards. The common nodes of the parallel branches were connected to the output of an amplifier. A function generator supplied the 100, 1000 and 10K frequencies. The current and voltage were measured with an oscilloscope to calculate power. The power was set at 5 W_{rms} and calculated daily for the 120 hour test period.

The cones were treated identically to those in the exploratory experiment except that nine caliper measurements were made on each cone before operation. The area measured was marked and remeasured after the completion of the operation. The cones were removed from their frames and measured again in the marked areas. The tensile samples were also used to run the stiffness test.

RESULTS PRESENTATION

EXPLORATORY EXPERIMENTATION

The mean of the test results of the exploratory experimentation are shown in Table 1. Appendix VI tabulates all test results from the exploratory experiment. Upon operation, the paper in the cones returned to and surpassed the original test results for tensile, TEA and elongation. Only the folding endurance did not return to the original value.

TABLE 1

EXPLORATORY EXPERIMENTATION

Mean of test results				
Age (years)	0	25	25	25
Frequency	0	0	100	10K
Tensile (kg)	8.0	6.7	8.7	9.1
% Elongation	5.7	4.2	5.8	6.5
TEA	.137	.100	.140	.160
Fold	121	84	75	95

PRIMARY EXPERIMENT

The mean values of test results run on the cones used in the primary experiment are given in Tables 2, 3, and 4. A complete summary of test results are given in Appendix VII. The unaged exploratory test results were used with additional test results for the 0 Hz calculations.

The primary test results confirmed the trends found in the exploratory experimentation. The folding endurance of the different groups were erratic. The decrease in stiffness was similar for each frequency evaluated. The caliper mea-

surements had a large standard deviation and no conclusions could be drawn. Appendix VII also contains the results of the caliper measurements.

TABLE 2

PRIMARY EXPERIMENTATION

Age - Hz	Tensile	% Elongation	TEA	Fold	Stiffness
0 - 0	8.2	7.99	.141	95	16.3
	.9	.93	.0228	26	3.7
0 - 100	9.04	9.59	.165	192	15.0
	2.18	.72	.0242	206	2.4
0 - 1K	8.62	8.40	.153	101	14.8
	1.21	1.18	.0308	36	3.7
0 - 10K	8.55	9.20	.164	136	14.4
	1.03	.67	.0240	66	2.5

TABLE 3

CALIPER VARIANCE

(Caliper before - caliper after operation X.001 IN)

Speaker	A	B	C	A
	1.68	.32	-.49	.166
Std. Dev.	2.51	1.02	1.31	.69

TABLE 4

CALIPER VARIANCE

(Inside vs. Outside Frame Measurement X.001 IN)

Speaker	E	A
	-.48	-1.50
Std. Dev.	1.47	2.45

Tensile, TEA and elongation each increased after operation. The increases

were substantially larger at the apex of the cones. However, only the apex and perimeter were tested at 100 and 1K Hz. Also the increases decreased with the higher frequencies. Only the folding endurance, elongation and TEA were significantly different using the f-test and 95% confidence limits.

The TEA was significantly lower at the 1K Hz and 0 Hz compared to the 100 Hz and 10K Hz. This also held true for the elongation and folding endurance.

DISCUSSION OF RESULTS

EXPLORATORY EXPERIMENTATION

A decrease in the strength and elasticity was expected after aging, however, the return to the original strength plus a substantial increase was unexpected. The expected result of aging was to accelerate the strength loss during operation. The data obtained from this experiment indicates that the tensile, TEA and elongation increase with operation. This implies that operation of the driver produces a stronger, more flexible cone.

To explain the increase in strength, the forming process and fiber rigidity will be examined. The cones are formed, pressed and then dried under constraint. During the drying of the cone, the water between the fibers evaporates most readily. Then the water between the bonding sites is reduced. The hydrogen bonds form, increase in strength, and hold the fiber in the network. After more water is removed, the fibers shrink, causing the bonds and network to strain. When all the excess water is evaporated, the network is fairly rigid. Therefore, when a strain is applied, the fibers can support the load or fail. After the stress developed in one location exceeds the total stresses the remainder of the specimen can withstand, the specimen ruptures.

The sonic vibrations in the cone during operation may increase the flexibility of the fibers. If the fibers were more flexible, they could distribute the strain more evenly across the specimen. With a decreased stress per area the specimen could absorb more tensile energy and yield a higher tensile strength without increasing the strength of the fibers or the bonded area. This hypothesis would explain the increase in tensile, TEA and elongation.

The method used to measure the power input makes it impossible to correlate the 100 Hz and the 10K Hz frequency levels. One problem was the impedance of

the voice coil changes at different frequencies. Therefore, each driver did not have the same dynamic resistance as measured at its operating frequency. Also, the RCA Volt Ohm meter measures AC volts at 60 Hz. The measurement at 100 Hz might have been reasonably accurate but, the 10K Hz measurement was definitely inaccurate.

The power was calculated daily to determine the variance of the power supply. The power remained constant during the entire experiment. This calculation also proved that the voice coils had not shorted out or fused.

Because of the unexpected results in the exploratory experiment, it was decided to eliminate the aging of the cones and to concentrate on the increase in test results during operation.

PRIMARY EXPERIMENTATION

A decrease in the physical strength and elasticity was expected after operation, with the larger decrease at the lower frequencies. Operation of the drivers was intended to decrease the folding endurance, tensile, TEA and elongation to exhibit the mode of failure. However, the test results imply that the larger shear strains cause a stronger and a more flexible cone. The elongation, folding endurance and TEA are significantly effected by frequency. The f-test was used with 95% confidence level to determine if the result was significant. The elongation and folding endurance were unquestionable while the TEA was extremely close.

All tests that were significant by the f-test responded similarly to the frequencies. The largest variance in the test results were observed in the 100 Hz set. The next largest variance was seen in the 10K Hz set. These results imply that between 1K Hz and 10K Hz the strains become slightly additive. The cones seem to be able to dissipate the strains applied at 1K Hz, causing the lowest shear and tensile stresses to be produced at this frequency.

A large difference between the test results of the apex and the perimeter

was noticed in the 100 and 1K Hz sets. The mean and standard deviation for all the test results are tabulated in Table 2. These were the only sets where the two separate areas were tested. All properties tested increased dramatically at the apex. A statistical analysis could not be run on the small data group. The results reinforce the hypothesis that the paper cones mode of response is similar to a viscoelastic material. The stresses generated must have been greater at the apex than at the perimeter to cause a larger variance in properties at the apex. It is impossible to say whether the increased stresses is caused by the smaller area at the apex or less of the applied energy having been dissipated. The results indicate that the paper should be able to deform and absorb energy.

The mean value of tensile test results appear to be controlled by the shear stress developed. However, the variance between different cones in one set was larger than the variance between sets. This was also true for the stiffness test results. If more drivers were available for experimentation, it would be possible to statistically confirm the tensile and stiffness results.

The results of the caliper measurements are inconclusive. The variance between the same area measured twice is larger than the measured difference before and after operation. The ridges of the cone and the shallow throat on the micrometer are the major causes of this error.

The power was calculated daily to determine if variances existed in the power supply. The calculations also checked for any change in inductance of the drivers. Neither varied during the operation of the drivers.

CONCLUSIONS

The application of sonic strains to a driver caused significant increases in the test results of elongation, folding endurance and TEA. The tensile and stiffness results increased with the greatest increase occurring at the lowest frequency. The lack of water makes the possibility for increased hydrogen bonding impossible. Therefore, the strains applied to the cone probably effected the fibers to change the test results. The results indicate that the fiber have become more flexible.

The elongation, folding endurance and TEA results for the 0 and 1K Hz sets were substantially different than the 100 and 10K Hz sets. These results imply that the 100 and 10K Hz sets have had more strains applied than the other sets. The higher strains at 100 Hz would substantiate the use of Ferry's shear stress equation. However, Ferry's equation does not explain the higher variance at the higher frequency. The increased results could come from the paper's inability to dissipate the first strain before a second is applied. This irregularity can be explained by Boltzmann superposition principle.

The increase in strength at the apex could be caused by the increased stresses per area or the lesser amount of energy dissipation closer to the apex.

RECOMMENDATIONS

Future studies should use larger diameter drivers without ridges in the cones. This would facilitate sample taking from the cone and increase the probability of accurate caliper measurements. A larger cone would also facilitate the determination of the strength dissipated, with respect to the area of the cone or the ability of the paper to dissipate the applied strains.

The determination of the period required to cause detrimental effects to the strength properties would be beneficial. After the strength properties decrease, the mechanics of the mode of failure could more readily be determined. This study could also determine when the decrease in strength properties effects the ability of the driver to produce undistorted sound. To improve high frequency response of the driver, future studies could investigate the additive effects of the applied strains and their effect to the strength properties.

Also, the effect of aging on the driver cones should be compared to the extended use of unaged drivers. This study could give further insight to the simulated aging of paper.

LITERATURE CITED

1. Horio, M. and Onogi, S., Journal of Applied Physics, 22 (7): 971 (1951).
2. Craver, J. K. and Taylor, D. L., Tappi, 48 (3): 142 (1965).
3. Kurath, S. F. and Rieman, W. P., Tappi, 47 (10): 629 (1964).
4. Ferry, J. D., "Viscoelastic Properties of Polymers" 2nd ed., New York, John Wiley and Sons, Inc., 1970, p. 31.
5. Barkas, W. W., in "Mechanical Properties of Wood and Paper", (R. Meredith, ed.), Amsterdam, North-Holland Publishing Co., 1952, p. 210.
6. Kaul, Dr. D., Professor of Physics, Western Michigan University, Interview, October 17, 1980.
7. Ferry, J. D., Op. Cit., p. 31.
8. Ibid., p. 136.
9. Ibid., p. 136.
10. Horio, M. and Onogi, S., Op. Cit., p. 974.
11. "CRC Handbook of Chemistry and Physics", (R. Weast, ed.), Boca Raton, Florida, 1979, p. E - 54.
12. Craver, J. K. and Taylor, D. L., Op. Cit., p. 143.
13. Craver, J. K. and Taylor, D. L., "Consolidation of the Paper Web", (F. Bolam, ed.), London Clowes and Sons Ltd., 1966, Vol. 1, p. 475.
14. Ferry, J. D., Op. Cit., p. 136.

APPENDIX I

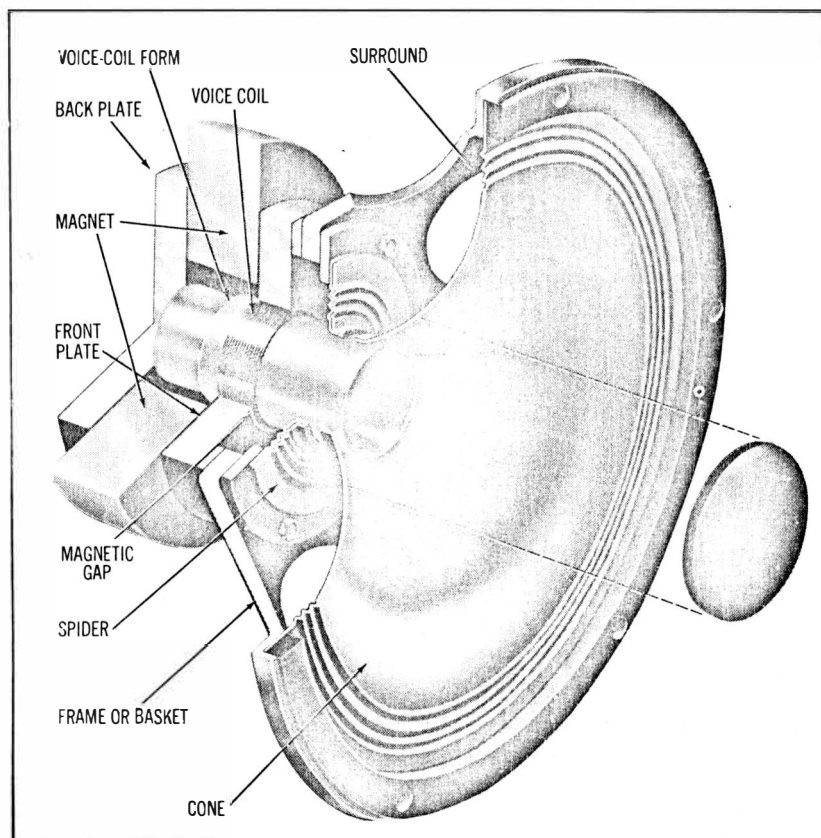


Fig. 1. A cutaway view of a conventional driver (full-range or low-frequency) showing the various internal parts. Other types of dynamic drivers, such as tweeters, contain essentially the same parts, although they differ somewhat in appearance and construction.

The conventional speakers (or more correctly called driver) are composed of components shown in Figure 1. The most prominent component, the diaphragm (speaker cone), is a shallow cone or rounded dome that is visible when the protective cover is removed from a loud speaker. Attached to the back of the cone or dome is a cylindrical bobbin, the voice-coil form. Around this cylinder is wound a coil of fine wire, the voice coil. The voice coil fits into a narrow circular slot assembly consisting of a permanent magnet and a surrounding structure of soft iron. The slot should be narrow in order to concentrate the magnet's field on the voice coil. A circular piece of corrugated fabric called a spider, is used to guide the movement of the voice coil so that it remains centered in the narrow slot of the magnet assembly.

APPENDIX II

DERIVATION OF SHEAR STRESS

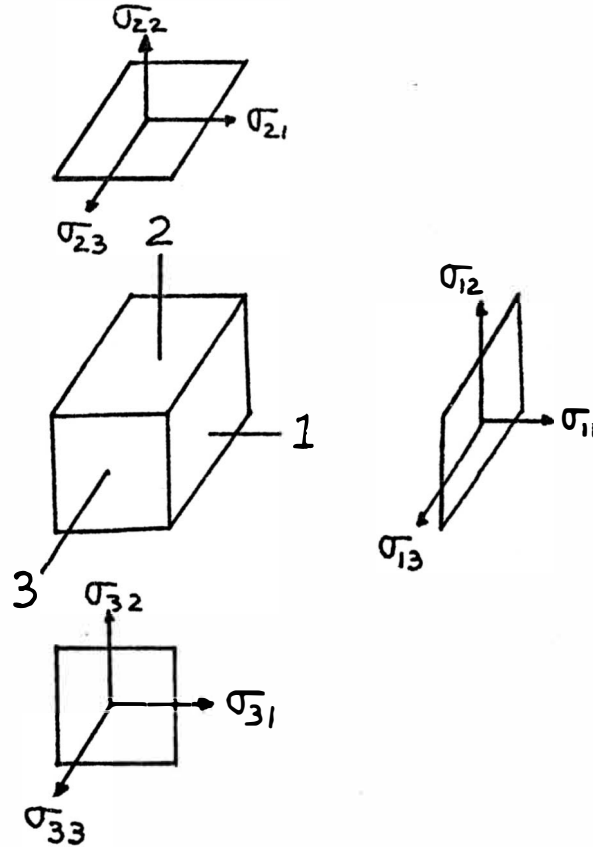


Figure 2. Identification Of The Components Of The Stress Tensor

In a viscoelastic body, the state of deformation at a given point is specified by a strain tensor which represents the relative changes in dimensions and angles of a small cubical section cut out at that position. The rate of strain tensor expresses the time derivatives of these relative dimensions and angles.

Similarly, the state of stress is specified by a stress tensor which represents the forces acting on the different faces of the cubical element from the different directions (see Figure 2).

The shear strain is applied parallel to the j direction. The force per unit

area is acting on the face of the cubical element which is perpendicular to i direction. The shear strain is equal to the following matrix:

$$\sigma_{ij} = \begin{pmatrix} \sigma_{11} & \sigma_{12} & \sigma_{13} \\ \sigma_{21} & \sigma_{22} & \sigma_{23} \\ \sigma_{31} & \sigma_{32} & \sigma_{33} \end{pmatrix} \quad (2)$$

In this case, the normal stresses σ_{ii} will be taken positive for tension and negative for compression. If the deformation is uniform, the stress and strain components do not vary with position. There are specific types of deformation in which stress and strain tensors assume a simple form. One of these is simple shear, shown in Figure 3.

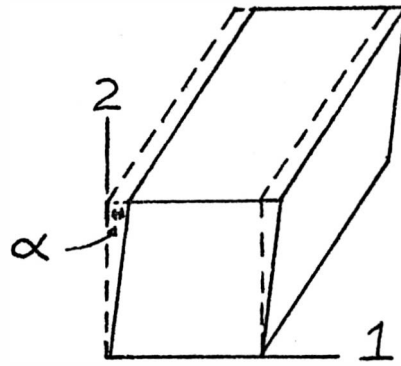


Figure 3. Illustration Of Simple Shear Of Cubical Element

In this figure the planes slide in the i direction, then the stresses and strains can be expressed as:

$$\gamma_{ij} = \begin{pmatrix} 0 & \gamma_{12} & 0 \\ \gamma_{21} & 0 & 0 \\ 0 & 0 & 0 \end{pmatrix} \quad (3)$$

where $\gamma_{21} = \gamma_{12}$, yields $\partial u_1 / \partial x_2 = \tan \alpha \approx \alpha$

then:

$$\sigma_{ij} = \begin{pmatrix} 0 & \sigma_{12} & 0 \\ \sigma_{21} & 0 & 0 \\ 0 & 0 & 0 \end{pmatrix} \quad (4)$$

The stresses and strains can readily be identified in Figure 2 and are functions of time.

APPENDIX III

DERIVATION OF SINUSOIDALLY APPLIED SHEAR STRESSES

Assuming that paper behaves as a viscoelastic material and the strain caused by the cone is sinusoidal in nature during operation, Ferry(7) has proven that the shear stress can be calculated with the following equation:

$$\sigma_{21} = \gamma (G' \sin \omega t + G'' \cos \omega t) \quad (1)$$

where: γ = maximum amplitude of strain
 σ_{21} = shear stress
 ω = frequency (radians/second)
 G' = shear storage modulus
 G'' = shear loss modulus.

To evaluate the stress equally for all frequencies, the integral will be solved for one-half a period and multiplied by twice the frequency in hertz. This will give the summation of the absolute value of tensile and compression stress developed for one second time period.

To continue the analysis of the shear stress, Ferry(8) has evaluated G' as:

$$G' = \frac{\omega^2 \lambda^2 \rho [4\pi - (\lambda/x_0)^2]}{[4\pi^2 + (\lambda/x_0)^2]^2} \quad (5)$$

where: λ = wavelength (cm)
 ρ = density (gm/cm³)
 x_0 = distance at which the amplitude drops by 1/e.

To evaluate the quantities inside the brackets, Ferry(9) stated that:

$$r = \frac{\lambda}{2\pi x_0} \quad (6)$$

Horio and Onogia(10) found r is approximately equal to 0.02 for most paper, and is acceptable to use when attenuation data is unavailable. Solving for λ/x_0 yields:

$$\lambda/x_0 = 2\pi r \quad (7)$$

$$= 0.04\pi \quad (8)$$

At the apex of the cone, λ would be equal to the wave being produced. At any other point away from the connection, λ would be controlled by the attenuation caused by the absorption of energy by the paper. In air, the velocity of sound (V_s) equals 366.05 m/s(11), which yields:

$$\lambda = \frac{1 \text{ second}}{\lambda \text{ cycle}} \left(\frac{36605 \text{ cm}}{1 \text{ second}} \right) = \frac{36605 \text{ cm}}{\lambda \text{ cycle}} \quad (9)$$

Craver and Taylor(12), who were pioneers in the paper sonics field, contend that only a fraction of the sheet can support a load and transmit sound. Therefore, the fiber substance density is the most appropriate value for density. They confirmed this by calendering a handsheet to twice its original density and measuring the sound velocity before and after. The calendering caused the velocity to raise by five percent only. They gave the density of cellulose as 1.55 gm/cm³(13). It is now possible to evaluate G' .

$$G' = \frac{\omega^2 \lambda^2 C [4\pi^2 - (\lambda/x_0)^2]}{[4\pi^2 + (\lambda/x_0)^2]^2} \quad (5)$$

$$= \frac{(2\pi \gamma)^2 (v_s/\gamma)^2 1.55[4\pi^2 - (0.04\pi)^2]}{[4\pi^2 + (\lambda/x_0)^2]^2} \quad (10)$$

$$= v_s^2 \times 1.548 \quad (11)$$

It is also possible to evaluate Ferry's(14) equation for G'' .

$$G'' = \frac{2 C v_s^2 r}{(1 + r^2)^2} \quad (12)$$

$$= \frac{2 (1.55) v_s^2 (0.02)}{[1 + (0.02)^2]^2} \quad (13)$$

$$= v_s^2 \times 6.195 \times 10^{-2} \quad (14)$$

Since the constant multiplied by G' is twenty five times greater than the G'' 's constant, the period of evaluation will be where the integral of G' is positive to give a maximum value of σ_{21} with the least number of integrals to solve. The value of σ_{21} can now be evaluated for one-half of a period.

$$\sigma_{21} = \gamma \left[\int_{t=0}^{t=\frac{180^\circ}{\omega}} (G' \sin \omega t + G'' \cos \omega t) dt \right] \quad (15)$$

$$= \frac{\gamma}{\omega} \left[G' \int_{t=0}^{t=\frac{180^\circ}{\omega}} \omega \sin \omega t dt + G'' \int_{t=0}^{t=\frac{180^\circ}{\omega}} \omega \cos \omega t dt \right] \quad (16)$$

$$= \frac{\gamma}{\omega} \left[G' (-\cos \omega t) + G'' (\sin \omega t) \right]_{t=0}^{t=\frac{180^\circ}{\omega}} \quad (17)$$

$$= \frac{\gamma}{\omega} (G') \quad (18)$$

Remembering that the amplitude is inversely proportional to the square of the frequency and $\omega = 2\pi \gamma$, equation 16 can be reduced to:

$$\sigma_{21} = \frac{G'}{2\pi \gamma^3} \quad (19)$$

Substituting in the calculated values of G' yields:

$$\sigma_{21} = \frac{v_s^2}{\sqrt[3]{}} \times 0.2464 \quad (20)$$

The normal tensile stress (σ_{22}) = $\frac{1}{2} \sigma_{21}$. Verification of this can be found in Appendix IV. The tensile stress is easily calculated as:

$$\sigma_{22} = \frac{v_s^2}{\sqrt[3]{}} \times 0.1232 \quad (21)$$

It is now possible to evaluate the shear and tensile stresses developed for half of period and for one second at the designated frequencies. The results are given in Table 5.

TABLE 5
SHEAR AND TENSILE STRESS AT APEX OF DRIVER

Frequency	(g/cm s)			
	Period		1 Second	
	$\frac{1}{2} \sqrt[3]{}$	$\frac{1}{2} \sqrt[3]{}$	$\frac{1}{2} \sqrt[3]{}$	$\frac{1}{2} \sqrt[3]{}$
Frequency	Shear	Tensile	Shear	Tensile
100	330	165	6.60×10^4	3.30×10^4
1K	3.30×10^{-1}	1.65×10^{-1}	660	330
10K	3.30×10^{-4}	1.65×10^{-4}	6.60	3.30

APPENDIX IV

THE RELATIONSHIP OF SHEAR STRAIN TO TENSILE STRAIN

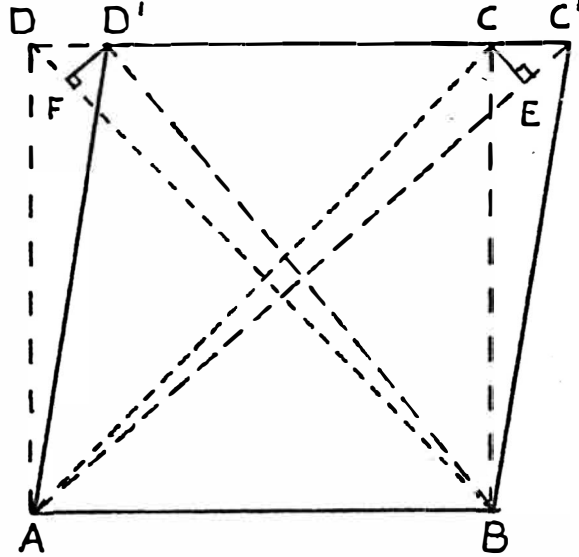


Figure 4. Body Deformed in Shear

The cross section of cube ABCD (Figure 4) is sheared as shown. Diagonals have been drawn for both conditions. The shear strain is equal to CC'/CB .

Construct the line CE which is perpendicular to the rhombus diagonal AC' . Since the strain is small, $\angle CC'E$ is close to 45° , and $C'E = CC'\sqrt{2}$. Similarly $AE \cong AC$. Now the tensile strain (\mathcal{E}) along AC' will be defined as:

$$\mathcal{E} = \frac{C'E}{AE} \quad (22)$$

$$= \frac{CC' / \sqrt{2}}{AC} \quad (23)$$

$$= \frac{CC' / \sqrt{2}}{CB \cdot \sqrt{2}} \quad (24)$$

$$= \frac{CC'}{2 CB} \quad (25)$$

$$\mathcal{E} = \frac{1}{2} \gamma \quad (26)$$

APPENDIX V

EXPERIMENTAL PROCEDURE

The drivers used were donated by Carbonneau Industries of Grand Rapids. They are used in tape recorders to listen to the recorded material. The five inch drivers are rated at $10 W_{rms}$ and labelled as 27 160 370-3.

EXPLORATORY EXPERIMENTATION

Three drivers were laid on wood strips and placed in an oven maintained at $105^{\circ}\text{C} \pm 0.5^{\circ}$ for 72 hours to simulate 25 years of natural aging. Immediately after the period ended, the drivers were enclosed in a desicator and transported to the test chamber. In the chamber, the drivers were removed from the desicator and allowed to equilibrate with the air, which was maintained at 76°F and 40% Rh.

The driver was mounted behind the center hole in a three-quarter inch piece of plywood. Five, five inch diameter holes were bored perpendicular to the surface in the pattern of five dots on a die. The upright piece of plywood was tilted slightly back and rigidly braced by two slats connected to a similar piece of plywood serving as a base.

The mounted driver was connected to the output of a 15W Gibson tube amplifier continuously for 120 hours. The sinusoidal wave input for the amplifier was supplied by a Jackson Audio Oscillator. The oscillator was set at 100 Hz for one driver and 10 K Hz for the other. The power was set at $9 W_{rms}$ and was calculated daily using the following equation:

$$P = V^2 / R \quad (27)$$

The voltage drop was measured across the driver with a RCA Volt-Ohm Meter. The resistance was calculated by measuring the voltage drop across the driver and

100 Ohm resistor connected in series to a function generator. A 1K Hz sinusoidal wave was provided by a Hewlett - Packard function generator. The resistance was calculated using Ohm's Law:

$$R_{\text{Driver}} = V_{\text{Driver}} / I_{\text{Driver}} \quad (28)$$

and using the same equation in a different form yields:

$$I_{\text{Driver}} = V_{100r} / R_{100r} \quad (29)$$

Substituting equation 29 into equation 28 gives:

$$R_{\text{Driver}} = V_{\text{Driver}} / (V_{100r} / R_{100r}) \quad (30)$$

The two operated drivers were placed with the unused aged driver and an unaged driver in the testing laboratory for 24 hours to equilibrate to the 60% RH air. The unused driver was used to determine the effects of the simulated aging. The cones were removed from their frame and cut into four 5.0 cm by 1.5 cm specimens for the tensile test. The tests were run on the Instron Tensile Tester with a TEA integrator attached. The beginning jaw gap was set at 4.0 cm and the crosshead speed used was 0.5 cm / min. The remainder of the cone was cut into 1.5 cm strips for the fold test. Since the fold specimens were less than two inches long, scotch tape was placed on both sides of the specimen above the tested area to reach the upper clamp. All tests were run according to Tappi Standard Procedure except as noted above.

PRIMARY EXPERIMENTATION

All drivers were placed in the testing chamber and allowed to equilibrate

to the 40% RH air. The caliper of the cones was measured at nine places using a one inch micrometer. The area measured was marked with a pencil. During the operation of the drivers, three parallel branches were made using two drivers in series. Since only enough drivers were obtained to allow five drivers to be operated at each frequency, the sixth driver was a previously used driver and taped from the apex to the frame to simulate the other drivers operating. The drivers that were being tested were mounted with screws securely behind the holes on the frame described in the exploratory experiment.

The common nodes of the parallel branches were attached to the eight ohm and ground outputs of one channel on a Harmon - Kardon Citation II amplifier. The input signal came from a Hewlett - Packard function generator. A half ohm resistor was placed between the common ground of the parallel branches and the amplifier ground to measure the voltage drop to calculate the current.

Generator Amplifier

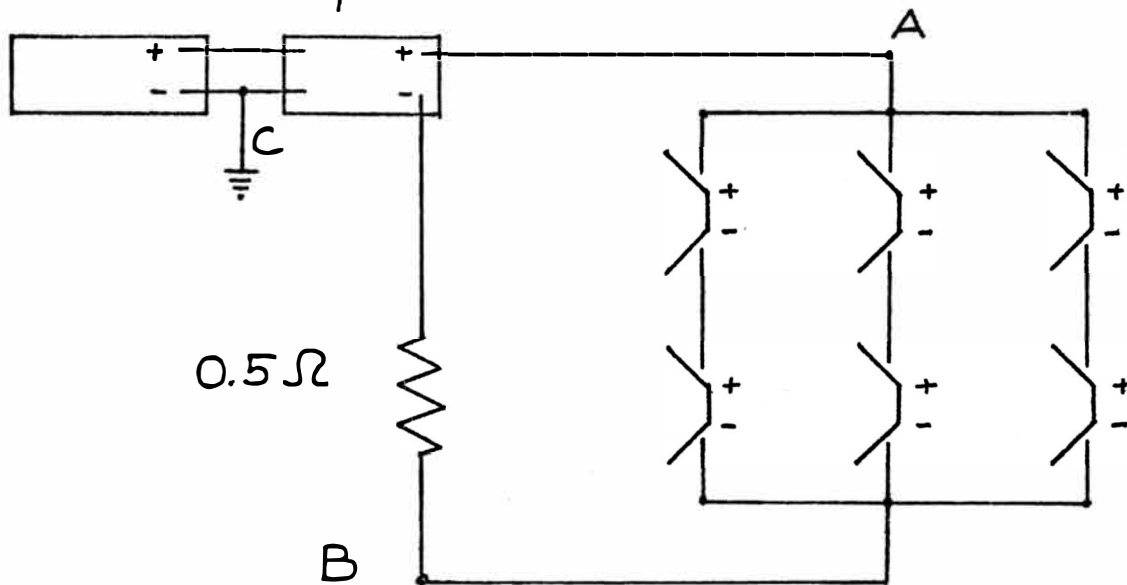


Figure 5

A schematic of the laboratory equipment set-up is shown in Figure 5. The first set of drivers were operated at 10K Hz and 5 W_{rms} (to each individual driver) for 120 consecutive hours. The second and third sets were operated at 100 Hz and 1K Hz repectively. Again, these frequencies represent average high, middle and low ranges of this driver's operation.

The total power was calculated by using the following equation:

$$P_T = \frac{1}{2} I_m V_m \cos \theta \quad (31)$$

where : P_T = total power

I_m = Maximum peak value of current

V_m = maximum peak value of voltage drop across drivers

θ = angle between I_m and V_m

To measure the needed values, point A was connected to channel A and point B was connected to channel B on a two channel Tektronics Ocilloscope. Channel A was also used as the trigger signal for the scope. The ground of the function generator (point C) was attached to the earth ground of the scope.

The voltage drop across the drivers was calculated by using the law of cosines on the voltage values from channel A and B. This equation is:

$$V_m = V_{AB} = \sqrt{V_A^2 + V_B^2 - 2 V_A V_B \cos \theta_{AB}} \quad (32)$$

where : V_{AB} = voltage at point A with respect to point B

V_A = voltage at point A with respect to ground

V_B = voltage at point B with respect to ground

$\cos \theta_{AB}$ = phase angle between V_A and V_B

To calculate the phase angle between V_A and V_B , channel A and B were centered on the ocilloscope screen. The distance between V_A abd V_B was measured and multiplied by 180° . This number was divided by the distance on the scope for channel A to complete 180° to give the angle in degrees.

The current supplied by the amplifier was calculated using Ohm's Law:

$$I_m = V_{.5\Omega} / R_{.5\Omega} \quad (33)$$

$$= 2 V_{.5\Omega} \quad (34)$$

$$= 2 V_B \quad (35)$$

Substituting equations 32 and 35 into equation 31 yields:

$$P_T = V_B \left(\sqrt{V_A^2 + V^2 - 2V_A V_B \cos \theta_{AB}} \right) \cos \theta_{AB}$$

The amplitude of the function generator was used to control the total power input. The power to each driver is calculated by dividing the total power by six. The rms power value is found by dividing the total power by the square root of two. The power was arbitrarily set at 5.0 W_{rms} and is within the normal operating range of this driver.

After the drivers were operated, they were unscrewed from the frame. The caliper of the previously marked areas were measured again. The cones were removed with a razor knife and the caliper measured again. The caliper was measured for the 10K Hz set only. The cones were conditioned and cut identically to the cones in exploratory experiment. The Taber Stiffness Test was run on the tensile specimens and tensile and fold were run as described in the exploratory experiment.

APPENDIX VI

EXPLORATORY EXPERIMENTATION TEST RESULTS

Condition	Tensile	% Elongation	TEA	Fold
0 - 0				
	8.7	6.6	ND	41
	7.6	5.9	.148	166
	7.9	6.2	.164	178
	7.8	4.3	.100	99
Mean	8.0	5.7	.137	121
Std. Dev.	.48	1.0	.033	63
25 - 0				
	7.0	4.7	.093	103
	6.9	3.9	.102	45
	6.5	3.5	ND	79
	6.7	4.7	.106	109
Mean	6.7	4.2	.100	84
Std. Dev.	.22	0.5	.00666	29

ND = No Data

	Tensile	% Elongation	TEA	Fold
Condition				
25 - 100				
	8.8	6.2	.151	75
	8.7	5.5	.138	63
	8.4	5.1	.118	75
	8.8	6.2	.156	86
Mean	8.4	5.8	.140	75
Std. Dev.	.19	0.4	.0169	9.4
25 - 10K				
	9.5	6.2	.162	43
	9.0	6.6	.141	138
	9.1	7.4	.182	79
	8.8	5.9	.154	120
Mean	9.1	6.5	.160	95
Std. Dev.	.29	0.5	.0172	42.6

APPENDIX VII

0 Hz					
Speaker	Tensile	TEA	% Elongation	Fold	Stiffness
A	8.7	ND	10.6	86	ND
	7.6	.148	9.4	114	ND
	7.9	.164	10.0	81	ND
	ND	ND	ND	123	ND
Apex	ND	ND	ND	126	ND
B	9.2	.185	8.8	103	14.5
	8.4	.157	8.2	130	13.5
	8.6	.136	7.6	46	14.0
	ND	ND	ND	ND	15.0
Apex	ND	ND	ND	92	ND
C	7.6	.133	8.2	74	17.5
	7.7	.112	8.8	50	12.5
	8.0	.134	8.2	104	24.0
	ND	ND	ND	ND	18.5
Apex	ND	ND	ND	109	ND
D	7.9	.104	5.6	ND	ND
	8.1	.157	8.1	ND	ND
	7.8	.131	8.7	ND	ND
E	8.1	.130	6.9	ND	ND
	9.0	.166	8.7	ND	ND
	8.7	.151	8.1	ND	ND
F	7.8	.100	6.9	ND	ND

100 Hz

Speaker	Tensile (kg./1.5cm)	TEA	% Elongation	Fold (Mit)	Stiffness (Taber/1.5cm)
A	7.9	.144	9.4	131	14.5
	ND	ND	ND	85	19.0
	ND	ND	ND	108	13.0
	ND	ND	ND	ND	13.0
Apex	ND	ND	ND	15.4	ND
B	9.6	.211	10.0	87	14.5
	9.0	.162	8.8	ND	14.0
	8.4	.165	10.0	ND	14.0
	ND	ND	ND	ND	17.5
Apex	ND	ND	ND	820	ND
C	9.0	.196	10.0	18.8	19.5
	9.2	.175	9.4	172	19.5
	ND	ND	ND	98	15.0
	ND	ND	ND	ND	12.0
Apex	ND	ND	ND	53.3	ND
D	8.6	.170	9.4	103	12.5
	7.3	.123	8.8	99	13.5
	8.8	.199	10.6	ND	13.0
	ND	ND	ND	ND	12.0
E	8.8	.166	9.4	125	15.0
	8.0	.150	9.4	104	14.0
	9.1	.178	9.4	76	15.5

1K Hz					
Speaker	Tensile	TEA	% Elongation	Fold	Stiffness
A	1.04	.170	ND	79	11.0
	8.7	.156	8.1	ND	13.5
Apex	11.4	.202	9.3	113	10.0
	10.1	.226	10.6	ND	11.0
B	6.7	.114	6.9	81	15.5
	ND	ND	ND	101	16.0
Apex	8.1	.161	9.1	117	20.0
	ND	ND	ND	ND	23.5
C	7.8	.137	7.5	108	18.0
	7.6	.138	8.1	123	13.0
	ND	ND	ND	80	ND
Apex	9.5	.179	9.9	92	10.5
	9.2	.170	9.3	ND	15.5
D	7.5	.142	8.1	131	13.5
	7.8	.121	7.5	ND	13.5
Apex	9.3	.177	9.3	154	15.0
	9.0	.157	8.0	ND	18.0
E	7.2	.125	6.2	100	17.0
	7.2	.114	6.9	66	19.5
	ND	ND	ND	141	ND
Apex	8.8	1.56	8.7	ND	9.0
	9.2	.176	9.3	ND	13.5

10 K Hz

	Tensile	TEA	% Elongation	Fold	Stiffness
Speaker					
A	8.8	.172	8.8	84	17.5
	9.5	.181	8.8	39	18.5
	10.2	.219	10.6	ND	16.5
	ND	ND	ND	ND	14.0
Apex	ND	ND	ND	201	ND
B	8.8	.155	9.4	154	14.0
	8.3	.146	8.8	115	13.0
	8.0	.142	8.8	229	8.0
	9.2	.172	8.8	ND	ND
C	7.7	.146	8.8	88	15.0
	7.1	.141	ND	60	12.5
	ND	ND	ND	ND	12.5
Apex	ND	ND	ND	124	ND
D	7.9	.161	10.0	89	15.0
	ND	ND	ND	73	15.5
	ND	ND	ND	31	13.5
	ND	ND	ND	ND	13.0
E	ND	ND	ND	208	13.0
	ND	ND	ND	ND	15.0
	ND	ND	ND	ND	16.5
	ND	ND	ND	ND	12.0

Test	F Calculated	Significant
Elongation	10.07	Yes
Folding Endurance	5.05	Yes
Stiffness	.385	No
Tensile	1.32	No
TEA	3.04	No

If the calculated F value is greater than 3.34, the probability is 95% that the frequency does have an effect on the property tested. The TEA would be significant at a 87% probability.

CALIPER - BEFORE vs. AFTER OPERATION

(X 0.001 IN)

Speaker	A			B		
	Before	After	Difference	Before	After	Difference
Position						
1	14.3	15.6	+1.3	15.7	17.4	+1.7
2	14.8	14.0	-0.8	16.8	17.5	+0.7
3	13.2	14.4	+1.2	18.8	17.7	-1.1
4	13.7	13.8	+0.1	18.0	16.8	-1.2
5	13.2	15.2	+2.0	16.5	16.7	+0.2
6	13.5	13.6	+0.1	15.2	15.3	+0.1
7	13.3	21.1	+7.1	16.2	16.6	+0.4
8	14.4	18.6	+4.2	10.2	10.6	+0.4
9	15.7	15.6	-0.1	11.5	13.2	+1.7
Mean		+1.68			+0.32	
Std. Dev.		2.51			1.02	
Speaker	C			D		
	Before	After	Difference	Before	After	Difference
Position						
1	15.6	14.2	-1.2	15.3	16.4	+1.1
2	16.8	16.7	-0.1	16.3	16.5	-0.2
3	15.8	15.6	-0.2	17.6	16.4	-1.2
4	15.5	15.4	-0.1	15.4	16.4	+1.0
5	15.2	15.6	+0.4	16.4	16.5	+0.1
6	15.8	12.1	-3.7	10.4	10.9	+0.5
7	15.1	15.4	+0.3	16.1	16.2	+0.1
8	17.6	18.2	+0.6	16.4	16.0	0.0
9	17.6	17.2	-0.4	15.5	15.2	-0.3
Mean		-0.49			+0.17	
Std. Dev.		1.31			0.69	

CALIPER - CONE IN vs. OUT OF FRAME

(X 0.001 IN)

Speaker	A			E		
	In	Out	Difference	In	Out	Difference
Position						
1	14.3	13.5	-0.8	14.7	16.1	+1.4
2	14.0	14.3	+0.3	19.0	15.8	-3.2
3	14.4	13.8	-0.6	13.4	13.7	+0.3
4	13.8	13.5	-0.3	13.8	13.5	-0.3
5	15.4	14.3	-1.1	14.3	14.2	-0.1
6	13.6	13.3	-0.3	13.9	14.5	-0.2
7	21.4	13.9	-7.5	14.2	14.4	+0.2
8	18.6	15.3	-3.3	17.1	14.6	-2.5
9	15.6	15.3	-0.3	14.8	14.1	-0.7
Mean		-1.50			-0.48	
Std. Dev.		2.45			1.48	